Available online at www.sciencedirect.com

ScienceDirect

Energy Procedia 74 (2015) 1410 – 1417

Energy Procedia

International Conference on Technologies and Materials for Renewable Energy, Environment and Sustainability, TMREES15

Study of thin film solar cells in high temperature condition

Mohamed Fathi[a*], Mahfoud Abderrezek[a], Farid Djahli[b], Mohammed Ayad[a]

[a]*Unité de Développement des Equipements Solaires, UDES/Centre de Développement des Energies Renouvelables, CDER, Bou Ismail, 42415, W. Tipaza, Algérie*

[b]*L.I.S Laboratory, Department of Electronic, Faculty of Technology, University of Setif 1, 19000 Setif, Algeria*

Abstract

In this paper, we study the effect of temperature on the Copper Indium Gallium Selenide (CIGS) thin film solar cells using the one dimensional solar cells simulator SCAPS-1D (Solar Cell Capacitance Simulator). The dependence of the CIGS solar cells characteristics on temperature was investigated from 25°C to 70°C at intervals of 5°C. We observed an apparent degradation in the open-circuit voltage and conversion efficiency with an increase of temperature from 25°C to 70°C, accompanied with degradation in the maximum power of the cell from 18.55 mW/cm^2 (25°C) to 14.941 mW/cm^2 (70°C). By the using of the luminescent downshifting approach, the conversion efficiency of the CIGS solar cell was enhanced under Standard Test Conditions (STC) at 25°C and in high ambient temperatures test conditions. The coefficient of the voltage variation to temperature $\Delta V_{oc} / \Delta T$ was reduced from -2 to –1.8 (mV/°C).

Peer-review under responsibility of the Euro-Mediterranean Institute for Sustainable Development (EUMISD)

Keywords: Solar cells, Simulation, CIGS, SCAPS-1D, Temperature, Luminescent Down-Shifting;

---

1. Introduction

The use of solar simulators has become necessary in the design and analysis of solar cells due to the complexity of the physical mechanisms that govern these photovoltaic devices [1]. The objective searched in the simulation of solar cells, is to find a relationship between the properties of the materials and the performances of the solar cell. In addition, it permitted us to identify physical and technological parameters that affect the solar cell performances during their operating at high ambient temperature.

---

* Corresponding author. Tel.: +213-542-116-181; fax: +213-24-41-04-84.
E-mail address: dr_fathimohamed@yahoo.fr

Peer-review under responsibility of the Euro-Mediterranean Institute for Sustainable Development (EUMISD)
doi:10.1016/j.egypro.2015.07.788

In the present research study, a numerical simulation of CIGS thin film solar cells has been carried out by using SCAPS-1D, developed at ELIS laboratory (Electronics and Information Systems) in GENT University, Belgium [2]. It was realized by Marc Burgelman et al. in ELIS department for the simulation of heterojunctions polycrystalline solar cells. It was first designed and used for testing CdTe and GIGS solar cells.

Because of their low cost of production and their high conversion efficiency [3-4], solar cells based on CIGS materials have been the subject of much recent research [5-6]. During their operation in external conditions, high ambient temperature plays a vital role and affects the performance of solar cells. This study becomes of paramount importance if we want to understand the behavior of CIGS solar cells in high temperature conditions. To enhance the energy conversion of photovoltaic cells and their behavior under high temperatures, we introduced a new approach based on luminescent down shifting (LDS) materials.

Nomenclature

SCAPS-1D	Solar Cell Capacitance Simulator one Dimension
TCO	Transparent Conductive Oxide
AM	Air Mass
QE	Quantum Efficiency (%)
J_{sc}	short circuit current density (mA/cm^2)
V_{oc}	open circuit voltage (Volt)
Pmax	maximum power (mW/cm2)
FF	Fill Factor (%)
Ŋ	Conversion efficiency (%)
LDS	Luminescent Down Shifting
PMMA	PolyMethyl Methacrylate
ASTM	American society for testing and material
STC	Standard Test Conditions

2. Studied structure

Figure1 shows a schematic diagram of the CIGS solar cell studied with Transparent Conductive Oxide TCO layer. The heterojunction is composed from CdS buffer layer (N) type and CIGS absorber layer (P) type. The thickness and doping level for several layers used in this structure are the same as those used by M. Gloeckler et al [7].

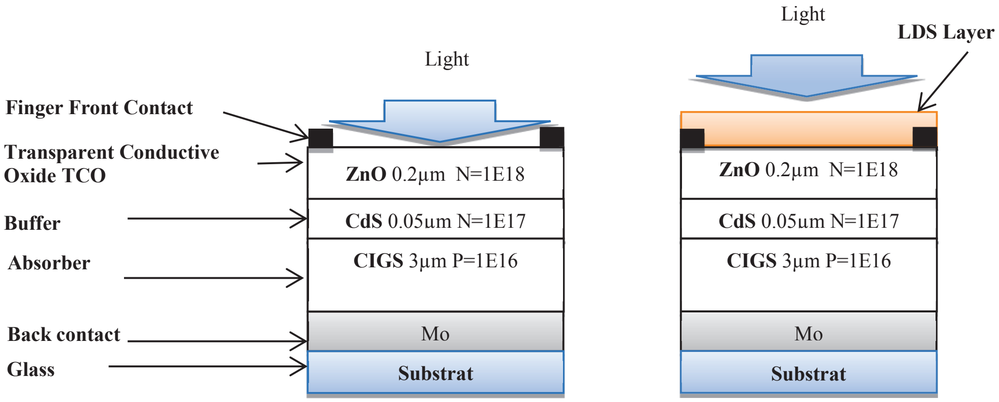

Fig. 1. The structure of the CIGS solar cell used for simulation with LDS (Left) and without LDS (Right).

Table 1. Main material parameters of ZnO/CdS/CIGS solar cell used in the simulation [7].

Semiconductor parameter's	**ZnO**	**CdS**	**CIGS**
Band gap (eV)	3.3	2.4	1.15
Dielectric permittivity (relative)	9	10	13.6
Electron mobility (cm²/Vs)	100	100	100
Hole mobility (cm²/Vs)	25	25	25
N_C effective density of states (1/cm^3)	2.2E18	2.2E18	2.2E18
N_V effective density of states (1/cm^3)	1.8E19	1.8E19	1.8E19
Electron thermal velocity (cm/s)	1E7	1E7	1E7
Hole thermal velocity (cm/s)	1E7	1E7	1E7
Front surface recombination velocity (cm/s)	1E7		
Back surface recombination velocity (cm/s)	1E7		
Front Reflectivity	0.05		
Back Reflectivity	0.8		

The performance of the CIGS hetero-junction solar cell was simulated under the standard spectrum AM1.5G at 25°C. The obtained results were in accordance with those of the literature (Table 2) [8].

Table 2. SCAPS1-D Simulation results of CIGS solar cell with experimental results.

Parameters	**CIGS (Experimental data) Ref [08]**	**CIGS SCAPS-1D Simulation**
V_{oc} (Volt)	0.678	0.666
J_{sc} (mA/cm^2)	35.22	34.866
FF (%)	78.65	79.88
η (%)	18.8%	18.50

2.1. CIGS Temperature effect simulation

After the calibration of the CIGS solar cell with reference [8], we explored the temperature effect on the CIGS solar cells performances by using the simulator SCAPS-1D.

Figures 2 (a) and (b) show the effect of ambient temperature on the Quantum Efficiency and the characteristics J (V) of CIGS solar cells. We observed a slight degradation of QE and short circuit current density J_{sc}, in comparison with the remarkable reduction of the open circuit voltage V_{oc}.

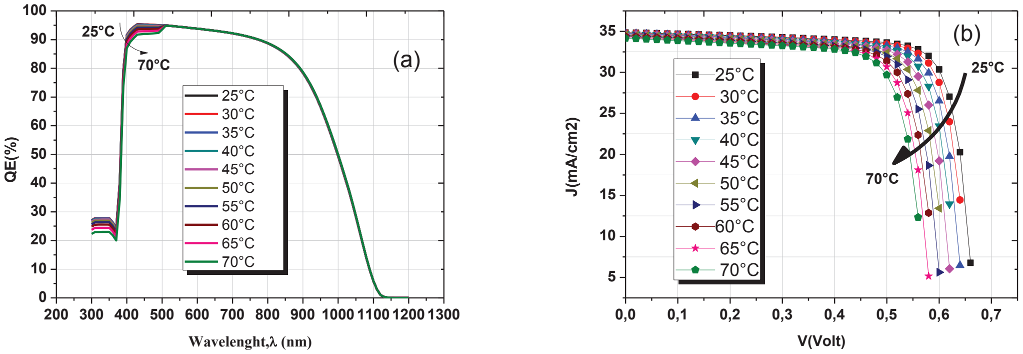

Fig. 2. Temperature dependence of the Quantum efficiency and the J(V) characteristics CIGS Solar cell.

Temperature effect on the on the CIGS solar cell performances (Jsc, Voc, ŋ, FF and maximum power of the cell) are showing in figure 3 and 4. A degradation in the open circuit voltage of the cell accompany by a degradation in the conversion efficiency and power of the cell. A slight variation observed in the short-circuit current and for factor.

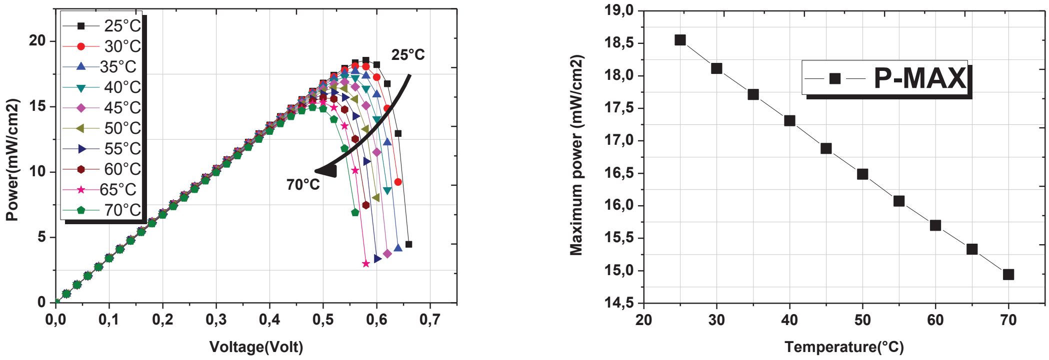

Fig. 3. Temperature dependence of P (V) and maximum power (Pmax) of CIGS Solar cell.

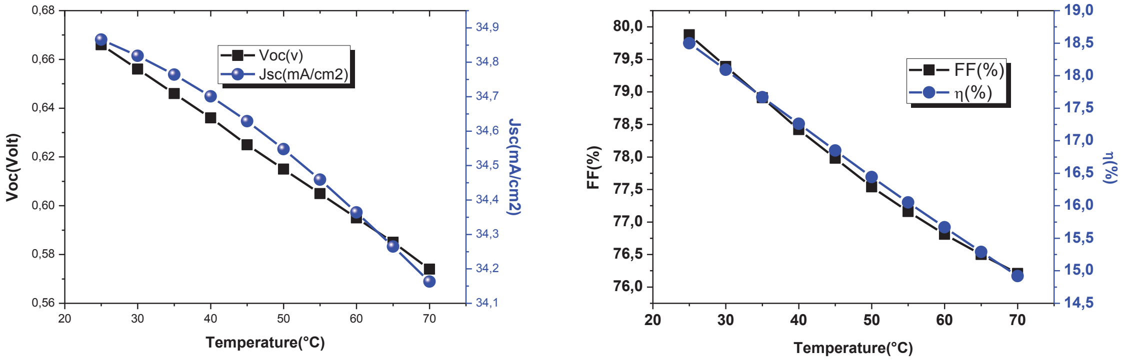

Fig. 4. Temperature dependence of V_{oc}, J_{sc}, FF and η of CIGS Solar cell.

Table 3. Performance of CIGS solar cell temperature coefficient.

Parameter's	**Value**
$\Delta V_{oc}/\Delta T$ (mV/°C)	-2
$\Delta J_{sc}/\Delta T$ (mA/cm2/°C)	-0,0162
ΔFF/ΔT (%/°C)	-0,088
Δη/ΔT (%/°C)	-0,082
$\Delta P_{max}/\Delta T$ (mW/cm2/°C)	-0.078

3. Enhancement of the CIGS solar cell performances

In this part and in the aim to enhance the conversion efficiency of the CIGS solar cell, the photovoltaic (PV) glass encapsulation material is replaced with a polymer material of polymethyl methacrylate (PMMA) type, doped with several kinds of organic dyes [9, 10]. The organics dyes move the photons from ultraviolet and blue region (where quantum efficiency of the cell is lower) to the visible region (where quantum efficiency of the cell is higher). This approach provides good adaptation between solar spectrum and spectral response of the solar cells; it also reduces the thermal losses in the solar cells [11].

We used, in this study, various samples of luminescent downshifting organics materials (LDS) formed by dyes mixed with PMMA. We will investigate the three fluorescent organic dyes (BASF Lumogen Violet 570 (V570), Yellow 083 (Y083), and Orange 240 (O240)) [13]. They are all made of napthalomide and perylene molecules, manufactured by BASF (Ludwigshafen, Germany). In this section we replaced the spectrum input in SCAPS-1D, AM1.5G (ASTM G173) by the modified spectrum $\Phi_{sae}(\lambda)$; this last is calculated from the amount of photons absorbed and emitted by dyes using the following expression :

$$\Phi sae(\lambda) = \Phi s(\lambda) - \Phi a(\lambda) + \Phi e(\lambda) \quad (1)$$

Where: $\Phi s(\lambda)$: is the incident solar spectrum
$\Phi a(\lambda)$: the amount of photons absorbed by dyes introduced in PMMA layer
$\Phi e(\lambda)$: the amount of photons emitted by dyes introduced in PMMA layer.

The amount of absorbed and emitted photons is calculated from the dyes absorption and emission Spectrum [10, 12]. Table 4 presents the different samples formed with organics dyes mixed with PMMA.

Table 4: The samples of dyes mixed with PMMA to form the three LDS layers [9].

Dyes Samples	Dyes	Absorption range (nm)	Emission range (nm)
S1	PMMA doped Violet 570	300-410	395-500
S2	S1+ Yellow 083	300-490	470-585
S3	S2+ Orange240	300-530	510-625

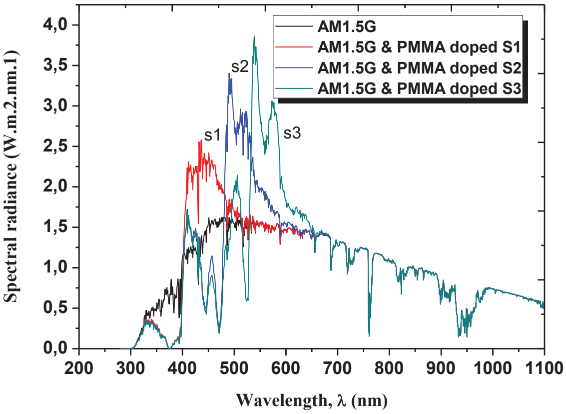

Fig. 5. Effect of luminescent dyes (S1, S2 and S3) on AM1.5G solar spectrum [10].

Figure 5 shows the LDS effect on the AM1.5G solar spectrum; we can observe the substantial modification on the incident AM1.5G Spectrum.

Table 5 summarizes the effect of LDS layers formed with different organics dyes on the CIGS solar cell performances. An increase in short currant density and conversion efficiency is observed with different samples used.

The gain in short-circuit current density and conversion efficiency is shown in table 6 and Figure 6, the gain in conversion efficiency can be increased to 6.5% with LDS doped S3.

Table 5: Simulation results of the CIGS solar cell with and without LDS layer for different sample types.

	CIGS (Experimental data) Ref [08]	CIGS SCAPS-1D Simulation	CIGS+LDS (S1)	CIGS+LDS (S2)	CIGS+LDS (S3)
V_{oc}	0.678	0.666	0.667	0.667	0.668
J_{sc}	35.22	34.866	36.389	36.589	36.893
FF	78.65	79.88	80.02	80.08	80.17
η	18.8%	18.50	19.18	19.48	19.71

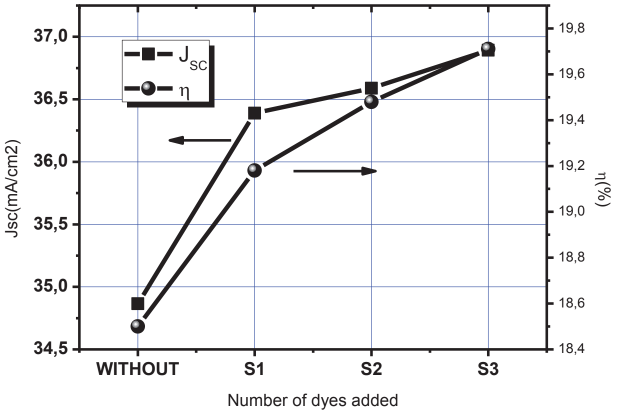

Fig. 6. Simulation results of the short circuit current density and conversion efficiency variation with number of dyes added.

Table 6. The Gain in short circuit current density and conversion efficiency of CIGS solar cells with the different samples used.

Gain	**LDS-S1**	**LDS-S2**	**LDS-S3**
Jsc(%)	4.368	4.941	5.813
ŋ(%)	3.675	5.297	6.540

Simulation results of CIGS solar cell J(V) characteristics with and without LDS PMMA layer are presented in Figure 7. The Figure 8 shows the normalized power of simulated results of CIGS cells with and without LDS materials compared with typical mulicrystalline silicon (mc-Si); CIGS thin films present higher power and improvement is added by LDS materials.

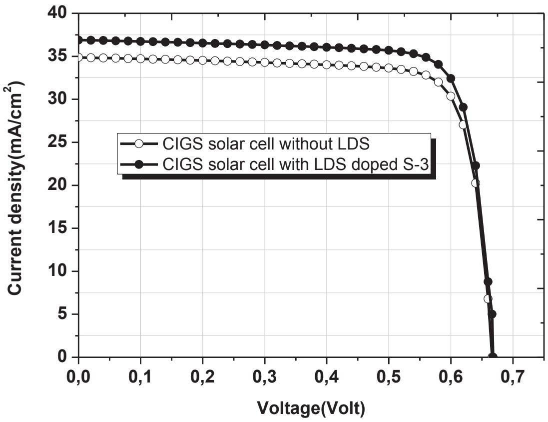

Fig. 7. Simulation results of CIGS solar cell characteristics with and without LDS PMMA layer.

3.1. Temperature effect on CIGS Solar cell with LDS PMMA layer doped S3

In this section we study the behavior of the CIGS solar cell with LDS layer doped S3. Table 7 presents the variation of CIGS solar cell performances with the temperature increasing.

The obtained results are given in Table 7. They concern the voltage coefficient, the short circuit current density, the fill factor and the conversion efficiency variation to temperature. All these variations are lower than those of CIGS without LDS layer (Table 8). A good adaptation between the solar spectrum and solar cell spectral response is obtained; this permitted to enhance the electrical and thermal solar cell performance.

Table 7. Temperature dependence of CIGS Solar cell performances with LDS (S3).

Temperature (°C)	**V_{oc}(v)**	**J_{sc} (mA/cm2)**	**FF(%)**	**ŋ (%)**
25	0.667	36.893	80.16	19.71
30	0.658	36.851	79.77	19.30
35	0.647	36.803	79.45	18.90
40	0.638	36.750	79.09	18.51
45	0.627	36.693	78.82	18.12
50	0.618	36.635	78.50	17.74
55	0.607	36.576	78.24	17.36
60	0.597	36.520	77.93	16.98
65	0.587	36.468	77.65	16.60
70	0.577	36.420	77.30	16.22

Table 8: The coefficient of V_{oc}, J_{sc}, FF and ŋ variation to temperature.

Parameter's	**CIGS without LDS**	**CIGS with LDS-S3**
$\Delta V_{oc}/\Delta T$ (mV/°C)	-2	-1.8
$\Delta J_{sc}/\Delta T$ (mA/cm2/°C)	-0,0162	-0.0116
ΔFF/ΔT (%/°C)	-0,088	-0.064
Δη/ΔT (%/°C)	-0,082	-0.076
$\Delta P_{max}/\Delta T$ (mW/cm2/°C)	-0.078	-0.075

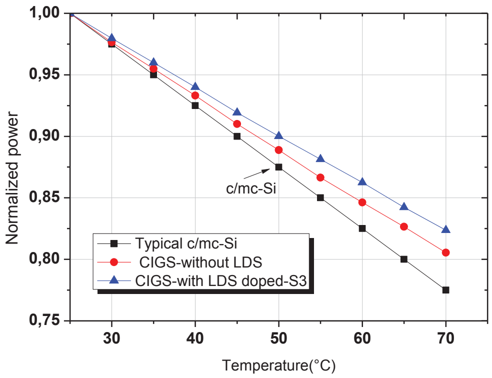

FIG. 8. Temperature dependence of Maximum Power (Pmax) of CIGS with and without LDS layer doped S3.

CONCLUSION

In this work, the CIGS solar cell performance was studied under high temperature conditions. The degradation was observed for the open voltage, conversion efficiency and power of the cell. By introducing the LDS layer on the top of CIGS solar cell, the electrical and thermal performances of the CIGS solar cell was improved in the standard and high temperature condition. The normalized power of CIGS cells with and without LDS materials shows better performances compared to conventional multicrystalline silicon cells.

ACKNOWLEDGMENT

The authors wish to thank Dr. M. Burgelman's group of Electronics and Information Systems (ELIS), University of Gent, for the SCAPS-1D program tool.

References

[01] T. Soga , "Nanostructured Materials for Solar Energy Conversion", First edition 2006, Elsevier.
[02] A. Niemegeers and M. Burgelman, "Effects of theAu/CdTe back contact on IV and CV characteristics of Au/CdTe/CdS/TCO solar cells," Journal of Applied Physics, vol. 81, Article ID 2881, 1997.
[03] M.A. Green,Third generation photovoltaics: ultra-high conversion efficiency at low cost, Prog. Photovolt.: Res. Appl. 9 (2001) pp. 123–135.
[04] R.M. Swanson, Photovoltaics power up, Science 324 (2009) pp. 891–892.
productions panning from PEC-cells to PV-electrolyzes : A comparison of efficiency, stability and device topology", Solar EnergyMaterials&SolarCells134 (2015), pp. 185–193
[05] Wei-Sheng Liu, Hung-Chun Hu, Nen-Wen Pu, Shih-Chang Liang "Developing flexible CIGS solar cells on stainless steel substrates by using Ti/TiN composite structures as the diffusion barrier layer", Journal of Alloys and Compounds, Volume 631, 15 May 2015, pp. 146-152.
[06] T. Jesper Jacobsson , Viktor Fjällström, Marika Edoff , Tomas Edvinsson, "CIGS based devices for solar hydrogen
[07] M. Gloeckler, A.L. Fahrenbruch, and J.R. Sites , "Numerical modeling OF CIGS and CdTe solar cells: setting the baseline", Photovoltaic Energy Conversion, 2003, Proceedings of 3rd World Conference on, Vol.1. pp. 491 - 494
[08] M.A. Contreras, B. Egaas, K. Ramanathan, J. Hiltner, A. Swartzlander, F. Hasoon, R. Noufi, "Progress Toward 20% Efficiency in Cu(In,Ga)Se2 Polycrystalline Thin-film Solar Cells ", Prog. Photovoltaics 7, 311, 1999.
[09] K. R. McIntosh and B. S. Richards, "Increased mc-si module efficiency using fluorescent organic dyes: a ray-tracing study", Photovoltaic Energy Conversion, Conference Record of the 2006 IEEE 4th World Conference on Vol. 2, Waikoloa, HI, IEEE, May 2006. pp. 2108 – 2111,
[10] M. Abderrezek, M. Fathi, F. Djahli, M. Ayad, "Study of the Effect of Luminescence Down-Shifting on GaAs Solar Cells With Several Optical Windows Layers", Journal of Solar Energy Engineering, February 2014, Vol. 136.
[11] David Ross, Efthymios Klampaftis , Jochen Fritsche, Michael Bauer, Bryce S. Richards, " Increased short-circuit current density of production line CdTe mini-module through luminescent down-shifting", Solar Energy Materials & Solar Cells 103 (2012), pp. 11–16.
[12] W. G. J. H. M. van Sark, "Simulating performance of solar cells with spectral downshifting layers," Thin Solid Films, vol. 516, no. 20, 2008. pp. 6808–6812